AIP Journal of Applied Physics

Tuning magnetic splitting of zigzag graphene nanoribbons by edge functionalization with hydroxyl groups

Huizhen Zhang, Sheng Meng, Haifang Yang, Lin Li, Huixia Fu, Wei Ma, Chunyao Niu, Jiatao Sun, and Changzhi Gu

Citation: Journal of Applied Physics **117**, 113902 (2015); doi: 10.1063/1.4915337
View online: http://dx.doi.org/10.1063/1.4915337
View Table of Contents: http://scitation.aip.org/content/aip/journal/jap/117/11?ver=pdfcov
Published by the AIP Publishing

Tuning magnetic splitting of zigzag graphene nanoribbons by edge functionalization with hydroxyl groups

Huizhen Zhang,[1] Sheng Meng,[1,2] Haifang Yang,[1] Lin Li,[1] Huixia Fu,[1] Wei Ma,[1] Chunyao Niu,[1] Jiatao Sun,[1,a)] and Changzhi Gu[1,2,b)]
[1]*Beijing National Laboratory for Condensed Matter Physics, Institute of Physics, Chinese Academy of Science, Beijing 100190, China*
[2]*Collaborative Innovation Center of Quantum Matter, Beijing, China*

(Received 24 December 2014; accepted 8 March 2015; published online 18 March 2015)

The electronic properties and relative stability of zigzag graphene nanoribbons are studied by varying the percentage of hydroxyl radicals for edge saturation using first principle calculations. The passivated structures of zigzag graphene nanoribbon have spin-polarized ground state with antiferromagnetic exchange coupling across the edge and ferromagnetic coupling along the edges. When the edges are specially passivated by hydroxyl, the potentials of spin exchange interaction across the two edges shift accordingly, resulting into a spin-semiconductor. Varying the concentration of hydroxyl groups can alter the maximum magnetization splitting. When the percentage of asymmetrically adsorbed hydroxyl reaches 50%, the magnetization splitting can reach a value as high as 275 meV due to the asymmetrical potential across the nanoribbon edges. These results would favor spintronic device applications based on zigzag graphene nanoribbons. © *2015 AIP Publishing LLC*. [http://dx.doi.org/10.1063/1.4915337]

I. INTRODUCTION

Zigzag graphene nanoribbons (ZGNRs) have attracted great research interests in recent years[1–5] because of its peculiar spin-polarized localized edge states,[6,7] from which many peculiar properties emerge. These states are localized along the edge direction and decay exponentially into the middle of the ribbons[8,9] and have nearly-flat energy level in the vicinity of Fermi level in the ground state. The potential shift of these edge states provides great possibilities for the ZGNR to be spin-selective material. Son *et al.*[3] found that when a transverse electric field is applied, the potentials of the localized edge states shift in opposite directions. Eventually, the ZGNR becomes half-metallic beyond a critical electric field. Other chemical decoration methods by adsorbing different functional groups on the two edges are proposed to generate half-metallic properties.[2] Due to the high carrier mobility[10–12] and the experimental success in product smooth and narrow (down to 10 nm)[13] zigzag ribbons, ZGNRs become promising candidates for spintronics applications in the future.[14,15]

Since the spin selective property is closely related to the edge states,[16–18] the adsorption of the functional groups in real growth environment can greatly influence the edge states and consequently the spin selective properties.[19] Although there are some studies on the edge structures[20,21] in atmosphere, as far as we know, there has few studies on how the electronic properties of ZGNRs are changed by a different ratio of distinct termination functional groups, possibly coming from the ambient conditions.

In this work, we use water vapor as an example of saturating environment to study the variation of the electronic structures of the zigzag graphene nanoribbons by adsorbing different concentrate of water residual groups on the edges. Since the dangling bonds of the zigzag graphene nanoribbon edges will be saturated by H/OH groups in the presence of water,[21] we use hydroxyl to represent the concentration of water in practical growth environment, which also contains other hydrocarbon gases. We found that with asymmetrically adsorbed hydroxyl, the potential difference of the two ZGNR edges can produce large spin splitting of the electronic bands. The maximum magnetization splitting is increasing when the asymmetry between the two edges gets greater, which can reach a large value of 275 meV, favoring room temperature spintronics applications. Therefore, this work implies that the influence of growth environment is a non-neglected factor. The better understanding and precise tuning of the spin selectivity properties can help us to achieve better performance of spintronic devices by the means of controlling water content in gaseous atmosphere or the pH value in solutions during ZGNR functionalization.

II. METHOD

The density function theory calculations were performed to investigate the electronic properties and magnetic structures of ZGNRs passivated by hydroxyl radicals and hydrogen as implemented in Vinnea Ab-initio Simulation Package (VASP) code. The Vanderbilt ultrasoft pseudopotential with the cutoff energy 420 eV is adopted to describe the interaction between electrons and ions. The generalized gradient approximation (GGA) is adopted to describe the exchange and correlation potentials. The special points sampling integration over the Brillouin zone is employed by using the Monkhorst-Pack method with a $1 \times 3 \times 1$ K-point mesh. In

a)Electronic mail: jtsun@iphy.ac.cn.
b)Author to whom correspondence should be addressed. Electronic mail: czgu@iphy.ac.cn.

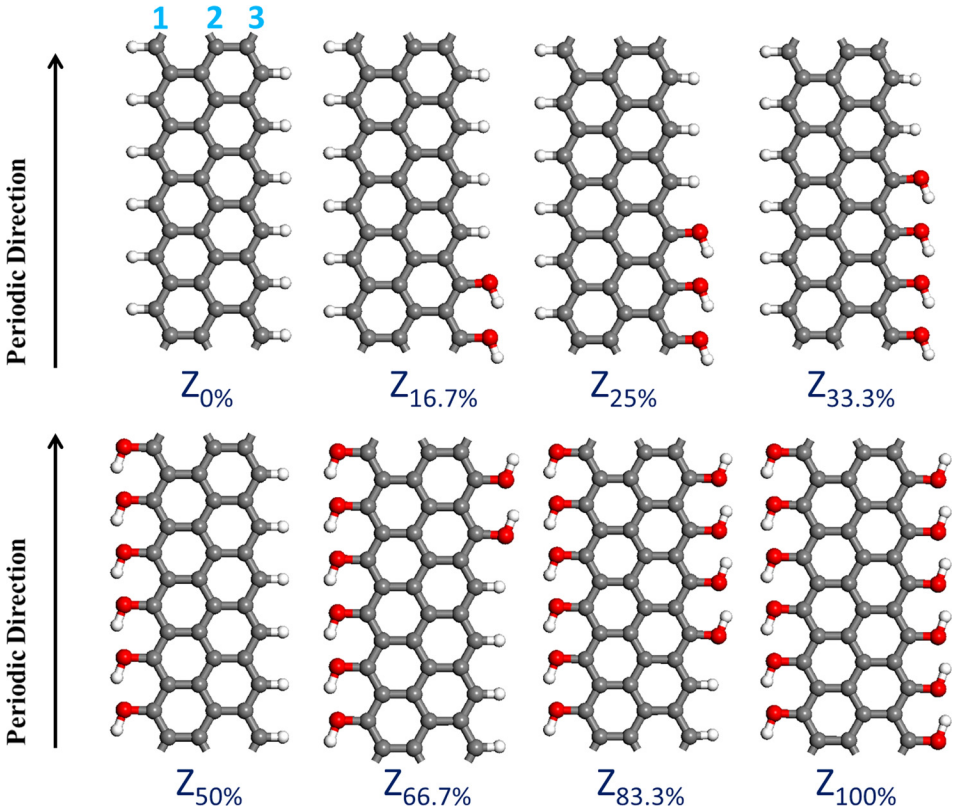

FIG. 1. Ball-and-stick models of the most stable structure for N = 3 ZGNR adsorbed with various concentration of hydroxyl radicals, where N is the number of carbon rows across the ribbon. Gray, red, and white balls denote carbon, oxygen, hydrogen atoms respectively. $Z_{X\%}$ is used to represent each structure, where Z represents zigzag nanoribbon, and x% represents the hydroxyl percentage.

our supercell setup, vacuum distance is about 15 Å between the ribbons laterally and vertically. The force tolerance for geometry optimization is 0.01 eV/Å for the maximum stress.

III. RESULTS AND DISCUSSION

We first chose a narrow zigzag ribbon with a finite width ~7 Å as shown in Fig. 1. The water content is represented by varying the relative ratio of hydroxyl radicals and hydrogen atoms. The hydroxyl concentration is 0%, 16.7%, 25%, 33.3%, 50%, 66.7%, 83.3%, 100%, respectively. After performing the geometry relaxation, we found that the most stable configuration for each hydroxyl concentration is the one with hydroxyls distributing asymmetrically and with all hydroxyls gathering together, as shown in Fig. 1. Here $Z_{X\%}$ is used to represent each structure, where Z represents zigzag nanoribbon, and x% represents the hydroxyl percentage.

The energy differences per unit cell for the hydroxyl passivated ZGNRs are calculated by taking into account of three spin configurations, nonmagnetic (NM), ferromagnetic (FM), and antiferromagnetic (AFM) states. For each configuration, the relative stability is $E_{AFM} < E_{FM} < E_{NM}$, indicating the occurrence of localized edge states in hydroxyl adsorbed ZGNRs, as shown in Fig. 2(a). Furthermore, with increasing the percentage of hydroxyl higher than 70%, the energy difference between the FM and AFM states is getting smaller indicating the possibility that the two states can be tuned by a small magnetic field.

The relative stability of all the configurations (shown in Fig. 1) in the ground state (AFM state) is also studied. Because of the different chemical compositions of each structure, the approach of calculating binding energy per

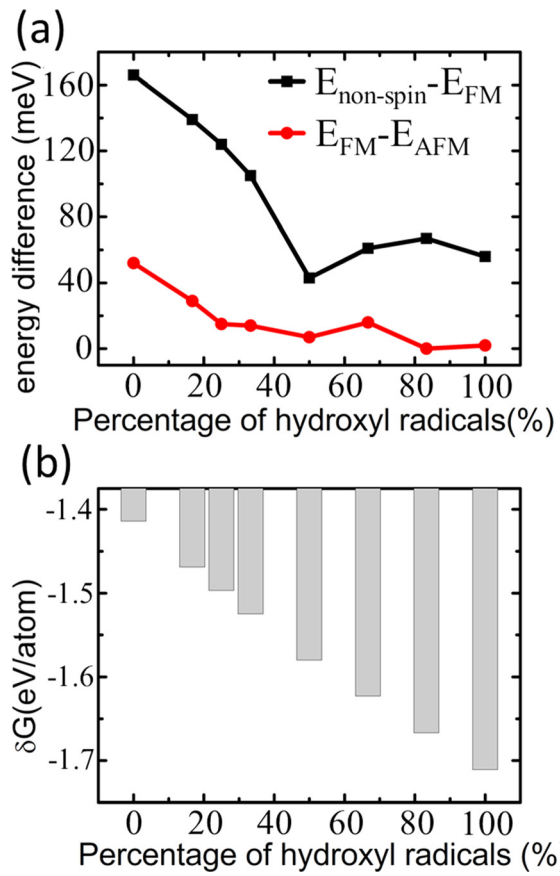

FIG. 2. (a) The energy differences between nonmagnetic and FM states (black line) and energy differences between FM and AFM states (red line) for each configuration (meV/unit cell). (b) Relative stability of the studied ZGNRs saturated by hydroxyl radicals (shown in Fig. 1). Negative values indicate stable structures with respect to each individual components in gas phase or graphene.

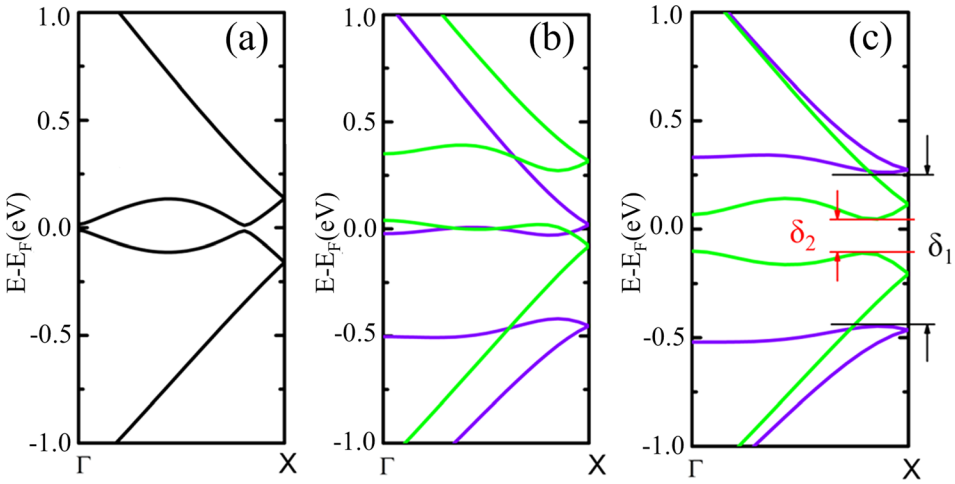

FIG. 3. Band structures of $Z_{50\%}$ for the (a) nonmagnetic, (b) ferromagnetic, and (c) antiferromagnetic states. The purple (green) line colors denote spin-up (spin-down) components. δ_1 (δ_2) are the band gaps for spin-up (spin-down) components.

atom does not provide a suitable measurement for comparing their relative stability. Therefore, we use the approach used in tertiary phase thermodynamics to account for chemical composition and to analyze the relative stability.[22,23]

According to this method, the Gibbs free energy δG for edge-modified ZGNRs is defined as

$$\delta G = E_C - n_H\mu_H - n_O\mu_O - n_C\mu_C, \quad (1)$$

where E_C is the cohesive energy per atom of chemically functionalized ZGNRs, and n_i is the molar fraction of atom $i(i = \mathrm{C},\ \mathrm{O},\ \mathrm{H})$ in the ribbons, satisfying the relationship $n_H + n_O + n_C = 1$. The binding energy per atom of H_2 and O_2 molecules are chosen as μ_H and μ_O, respectively, and μ_C is the cohesive energy per atom of graphene. The definition in this method allows for direct energy comparison between these functionalized nanoribbons with different compositions.

The relative stability of the ground states (AFM state) of the six configurations is shown in Fig. 2(b). We find that all the structures are stable, and more hydroxyl radicals passivated on the edges lead to more stable structures. This increasing stability comes from the increasing hydrogen bonds formed between adjacent hydroxyl groups.

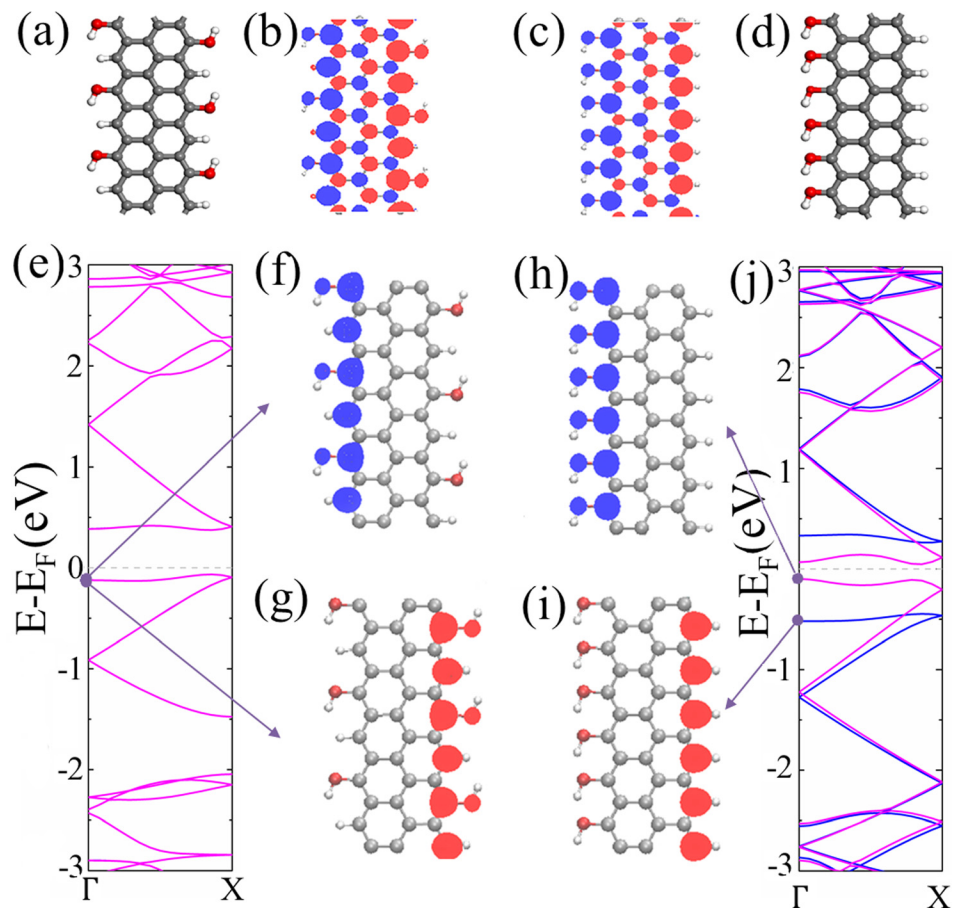

FIG. 4. Band structures and spin densities of the ZGNR ($Z_{50\%}$) with symmetrical and asymmetrical configurations of hydroxyl adsorption. (a) and (d) are ball-and-stick models for the symmetrical (a) and asymmetrical configuration (d). (b) and (c) are spin densities for (a) and (d), respectively. (e) and (j) are band structures for (a) and (d), respectively. (f)–(i) are the partial spin density of each corresponding state.

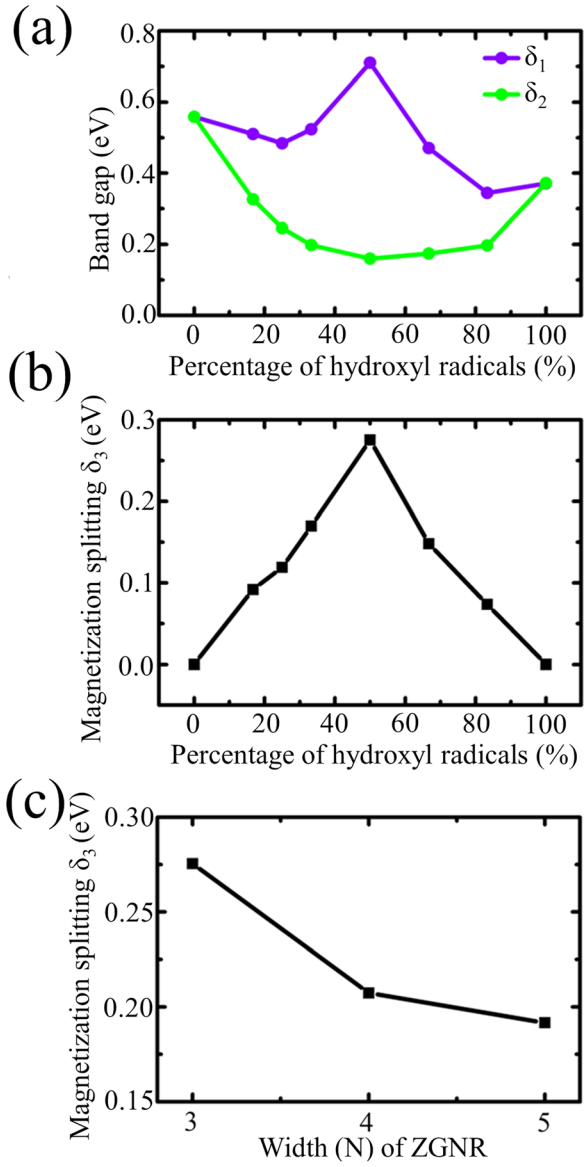

FIG. 5. (a) The band gap evolution of two spin components (δ_1 and δ_2 as defined in Fig. 3(c)) in hydroxyl adsorbed ZGNRs. (b) Spin magnetization splitting ($\delta_3 = |\delta_1 - \delta_2|/2$) of the hydroxyl adsorbed ZGNRs as a function of the hydroxyl concentration. (c) The width dependence of the spin magnetization splitting δ_3.

In Fig. 3, we present the band structures for $Z_{50\%}$ of three spin configurations, nonmagnetic (Fig. 3(a)), ferromagnetic (Fig. 3(b)), and antiferromagnetic states (Fig. 3(c)). In the FM states, the two degenerate bands in nonmagnetic state split as the hydroxyl groups are asymmetrically distributed on the two edges. In the AFM state (ground state), the band gap of one spin component becomes larger, leaving only one spin component in the vicinity of Fermi level, as shown in Fig. 3(c). We focused on the origin of this spin splitting and the influence of the variation of hydroxyls percentage on this spin splitting in the following.

Figure 4 shows the spin densities of the $Z_{50\%}$, with the hydroxyl symmetrically (Fig. 4(a)) and asymmetrically (Fig. 4(b)) distributed on the two edges. The asymmetrical configuration is more stable than the symmetrical one with an energy of about 955 meV lower per supercell. Both the two configurations exhibit a spin-polarized AFM ground state (Figs. 4(b) and 4(c)), similar to the fully hydrogenated ZGNR. When the hydroxyls distribute asymmetrically, the spin densities are also asymmetrical, and the corresponding band of the two states is split (Fig. 4(j)) forming a spin semiconductor. This implies that the spin splitting comes from the asymmetrical adsorption of hydroxyl and hydrogen along the two edges, which results in larger electrostatic potential along the lateral width.

The effect of hydroxyl concentration on the electronic structures of ZGNRs is summarized in Fig. 5. When the edges are symmetrically modified, the spin-up and spin-down bands are degenerate; when they are asymmetrically distributed, the spin splitting occurs where the two spin-polarized gaps have opposite response to the increase of hydroxyl content due to the presence of in-plane electrostatic potential. When the asymmetric potential difference becomes larger, the magnetization splitting (defined as $\delta_3 = |\delta_1 - \delta_2|/2$, where δ_1 and δ_2 are band gap for each spin component, respectively, as shown in Fig. 3(c)) reaches the maximum value, as shown in Fig. 5(b). The maximum spin splitting is $\delta_3 = 275$ meV.

To investigate how the spin magnetization splitting δ_3 is affected by the width of the ZGNRs, we use the asymmetric $Z_{50\%}$ ZGNR as an example. The corresponding relationship of maximum spin magnetization splitting and the ribbon width is presented in Fig. 5(c). With the increase of the ribbon width, the spin magnetization splitting decreases, indicating the decrease in the lateral electrostatic potential.

IV. CONCLUSIONS

In conclusion, the effects of hydroxyl concentration variation on the electronic properties and relative stabilities of the zigzag graphene nanoribbons are studied. All the structures passivated by hydroxyls studied in this work have a spin-polarized ground state with antiferromagnetic exchange coupling across the ribbon width. When passivated asymmetrically by hydroxyls, the potentials of the two edges become different and finally results in spin splitting in the bands. With increased asymmetry between the two edges, the spin splitting becomes larger and can reach 275 meV when the percentage of hydroxyl is 50%. It is shown that the variation of the water content can change the spin splitting of the zigzag ribbons, suggesting the significance of environment effect. The small energy difference between FM and AFM states for OH concentrations higher than 70% allows for tuning between spin semiconductor (AFM) and spin half-metal (FM) phases by applying a small magnetic field. This result highlights the potential capabilities of graphene nanoribbons for spintronics applications. This work provides a guidance to experimentalists on achieving room temperature spin semiconducting or half-metallic states based on zigzag graphene nanoribbons for spintronic applications.

ACKNOWLEDGMENTS

The authors thank MOST (2012CB921403 and 2013CBA01600), the National Natural Science Foundation of China (Grant Nos. 61390503, 51272278, 91323304, 61306114), and XDB07030100.

[1]D. Gunlycke, J. Li, J. W. Mintmire, and C. T. White, Appl. Phys. Lett. **91**, 112108 (2007).
[2]E. J. Kan, Z. Li, J. Yang, and J. G. Hou, J. Am. Chem. Soc. **130**, 4224 (2008).
[3]S. Young-Woo, M. L. Cohen, and S. G. Louie, Nature **444**, 347 (2006).
[4]K. N. Kudin, ACS Nano **2**, 516 (2008).
[5]O. Hod, V. Barone, J. E. Peralta, and G. E. Scuseria, Nano Lett. **7**, 2295 (2007).
[6]G. Z. Magda, X. Z. Jin, I. Hagymasi, P. Vancso, Z. Osvath, P. Nemes-Incze, C. Y. Hwang, L. P. Biro, and L. Tapaszto, Nature **514**, 608 (2014).
[7]A. Yamashiro, Y. Shimoi, K. Harigaya, and K. Wakabayashi, Phys. Rev. B **68**, 193410 (2003).
[8]K. Wakabayashi, M. Fujita, H. Ajiki, and M. Sigrist, Phys. Rev. B **59**, 8271 (1999).
[9]Y. Miyamoto, K. Nakada, and M. Fujita, Phys. Rev. B **59**, 9858 (1999).
[10]K. S. Novoselov, A. K. Geim, S. V. Morozov, D. Jiang, Y. Zhang, S. V. Dubonos, I. V. Grigorieva, and A. A. Firsov, Science **306**, 666 (2004).
[11]Y. B. Zhang, Y. W. Tan, H. L. Stormer, and P. Kim, Nature **438**, 201 (2005).
[12]C. Berger, Z. Song, X. Li, X. Wu, N. Brown, C. Naud, D. Mayou, T. Li, J. Hass, A. N. Marchenkov, E. H. Conrad, P. N. First, and W. A. de Heer, Science **312**, 1191 (2006).
[13]R. Yang, L. Zhang, Y. Wang, Z. Shi, D. Shi, H. Gao, E. Wang, and G. Zhang, Adv. Mater. **22**, 4014 (2010).
[14]O. V. Yazyev and M. I. Katsnelson, Phys. Rev. Lett. **100**, 047209 (2008).
[15]A. Dankert, M. V. Kamalakar, J. Bergsten, and S. P. Dash, Appl. Phys. Lett. **104**, 192403 (2014).
[16]M. Fujita, K. Wakabayashi, K. Nakada, and K. Kusakabe, J. Phys. Soc. Jpn. **65**, 1920 (1996).
[17]K. Nakada, M. Fujita, G. Dresselhaus, and M. S. Dresselhaus, Phys. Rev. B **54**, 17954 (1996).
[18]J. Guo, D. Gunlycke, and C. T. White, Appl. Phys. Lett. **92**, 163109 (2008).
[19]K. Jun, W. Fengmin, and L. Jingbo, Appl. Phys. Lett. **98**, 083109 (2011).
[20]L. Geunsik and C. Kyeongjae, Phys. Rev. B **79**, 165440 (2009).
[21]A. P. Seitsonen, A. M. Saitta, T. Wassmann, M. Lazzeri, and F. Mauri, Phys. Rev. B **82**, 115425 (2010).
[22]V. Barone, O. Hod, and G. E. Scuseria, Nano Lett. **6**, 2748 (2006).
[23]T. Dumitrica, M. Hua, and B. I. Yakobson, Phys. Rev. B **70**, 241303 (2004).